SMAR 2017 – Fourth Conference on Smart Monitoring,
Assessment and Rehabilitation of Civil Structures

SMAR 2017

Experimental and numerical study on the bond slip laws of adhesively bonded FRPs

Roman Sedlmair[1], Bernhard Walendy[2], Lothar Stempniewski[3]

[1, 2, 3] Karlsruhe Institute of Technology Institute of Reinforced Concrete and Building Materials – Department Reinforced Concrete, Karlsruhe, Germany

ABSTRACT: Post-strengthening of reinforced concrete (RC) with externally bonded fiber-reinforced polymers (FRP) has become very attractive and the number of applications is constantly increasing. Widely used is an epoxy based adhesive to bond the FRP to the surface of the concrete. Due to the stiff behavior of the adhesive the debonding occurs in the concrete top surface over a very short length. To calculate the debonding load a bond-slip law is taken into account.

The present paper focuses on the study on the bond stress-slip laws for externally bonded FRPs. Single lap-shear pull test series with varying bond lengths are performed, four different adhesives (one stiff and three soft) are used. The inferred bond stress-slip laws are implemented in a MATLAB® algorithm to calculate the debonding load, the maximal bearable load for certain bond lengths and the bond stress distribution over the bonded length. The results are discussed to demonstrate the potential for optimization by the use of a softer adhesive for strengthening RC with FRPs.

1 INTRODUCTION

Strengthening of concrete with externally bonded (EB) fiber reinforced polymers (FRP) is a well-known technique. FRP is a composite material made of a matrix (polymer) reinforced with fibers. Epoxy is generally used on the matrix phase. Various types of fibers are used, mainly Carbon (C) and Glass (G). FRP materials are available in different forms; unidirectional strips, sheets or fabrics with fibers in one or several directions.

Epoxy based adhesives are often used to bond the FRP on the (roughened) surface of the concrete. A drawback of this technique that it is not possible to mobilize the full tensile strength of the FRP due the low tensile strength of the concrete. The typical failure is the removal of a thin layer of concrete. Furthermore, stress concentrations (shear and normal direction) occur in the bonded zone next to cracks due to the high stiffness of the epoxy. These are the two main reasons for the premature failure of EB FRP for strengthening. One way to improve existing strengthening techniques is to create a more compatible system. In this paper, softer adhesives which activate a larger bonded zone and reduce stress concentrations are tested. In this way, a larger percentage of the tensile strength of the FRP can be utilized and the ultimate load carried by the FRP strengthening system increases (Kwiecień (2014)). Several researchers like Fitton et al. (2005) and Derkowski et al. (2010) described this effect before. According to them, two approaches have

to be taken into account for the usage of flexible adhesives. Firstly, if the adhesive has a higher strength than the surface/substrate it is bonded on, the strength of the structure is increased by the flexibility of the adhesives and the reduction of stress concentrations. The peak of stress concentration is directly related to the stiffness of the adhesive. The stiffer the adhesive, the higher is the peak of stress concentration. Secondly, if the used adhesive is of lower strength than the substrate, no more damage occurs in the substrate. This effect protects the FRP against failure, even if such failure eliminates ultimately the strengthening action, too.

This paper presents an experimental and numerical study on the bond behavior of EB FRP materials. Single-shear pull tests with four different adhesives (one stiff and three soft) were performed. The effect of the stiffness of the adhesive and bond length on bond behavior were investigated to infer the local bond-slip law and to calculate the interface fracture energy. To examine the limit of the adhesive the carbon sheets were directly wet lay-up bonded on high strength repair mortar. This is based on the second approach Derkowski et al (2010) described before. To show the possible advantages of using a softer adhesive and to calculate the debonding load the local bond-slip laws were implemented in an MATLAB algorithm. The strains and slips over the bonded length were calculated.

2 EXPERIMENTAL WORK

Pictures of the experimental setup are shown in figure 1. The experimental machine is a Zwick/Roell Z010. All tests were performed with 0.5mm/min and a data recording rate of 10 Hz. The aim of the experimental work was to examine the influence of differing adhesives and to infer their local-bond slip laws. The experimental setup and analysis approach of this single lap-shear pull test is described in detail in Walendy et al (2017). In contrast to this work, the FRP is bonded with the same adhesive on both sides, the analysis approach had to be adapted to this circumstance. Elongation between the two pieces of substrate was measured with two LVDTs, placed on the left and right hand side of the metallic cuboids. The slip obtained from elongation date was crosschecked with the measured displacement of the testing machine.

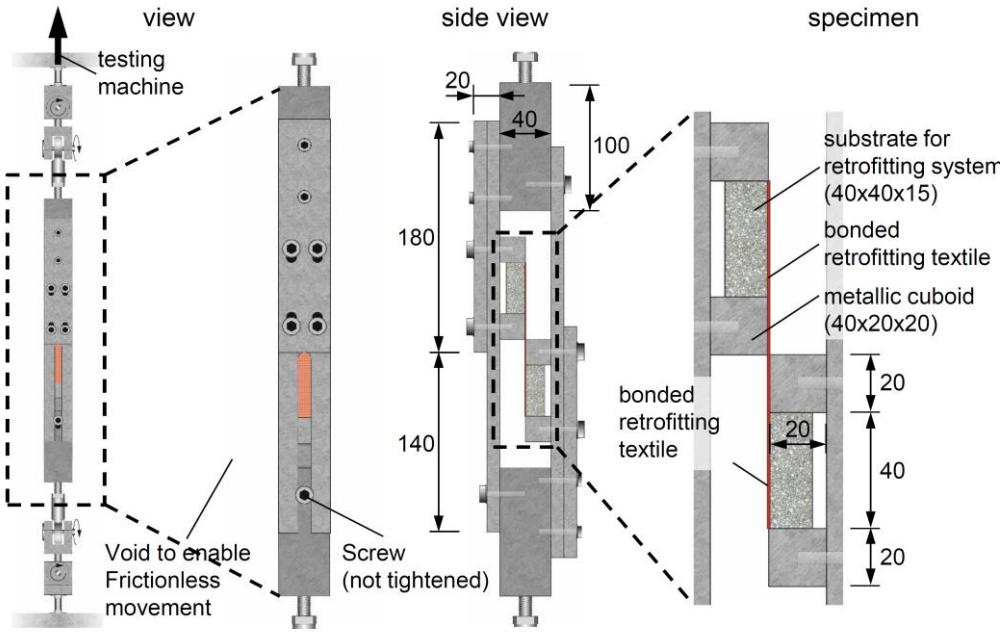

Figure 1. Experimental setup

The unidirectional Carbon sheet (A = 5mm², width 40 mm, Youngs Modulus 238.000 N/mm², ε_u = 1.8 %) was bonded 40 mm, 60 mm and 80 mm on high performance repair mortar ($f_{cm} \geq 48$ N/mm², $f_{ctm} \geq 3.8$ N/mm²). Three tests per adhesive and bonded length were performed. The mechanical properties (where available) are listed in Table 1.

Table 1. Mechanical properties of tested adhesives

	MC-DUR 1209	PU 1	PU 2	PU 3
Type	Epoxy	1K-PU	2K-PU	2K-PU
Youngs modulus [N/mm²]	3.000	3 ÷ 6	160	146
Tensile Strength [N/mm²]	-	5.25	-	24
Shear Strength [N/mm²]	-	1 ÷ 2	61	56
Elongation [%]	< 4	600	> 200	460
Adhesion to concrete [N/mm²]	14	-	3.64	4.66

2.1 Results

The mean maximum force measured in the experiments are listed in Table 2. According to Kwiecień (2014) all the PU adhesives are suitable to use them for flexible joints due to their low Young's modulus, high deformability and their elasto-visco-plastic behavior. Pictures of the FRP after failure (epoxy bonded FRP cohesion failure, all PU bonded FRPs adhesion failure) are shown in figure 2

Table 2. mean maximum force [N] and CoV

Type	MC-DUR 1209		PU 1		PU 2		PU 3	
	Force	CoV	Force	CoV	Force	CoV	Force	CoV
40 mm	6943	0.148	1193	0.021	4170	0.061	2379	0.086
60 mm	8098	0.123	-	-	5030	0.008	-	-
80 mm	8302	0.083	2267	0.029	7796	0.053	4138	0.222

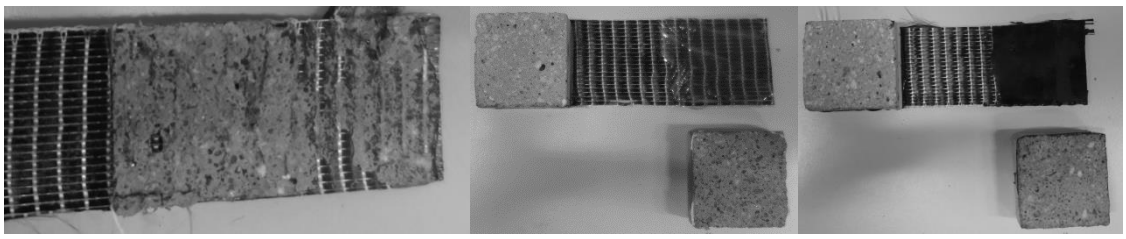

Figure 2. FRP after failure, bonded with epoxy (left), PU 2 (middle) and PU 3 (right).

2.2 Results compared to CNR-DT 200 R1/2013

The values of table 2 can be compared to the maximum force F_{max} calculated with equations 1 and 2. The effective bond length (or optimal bond length) l_{ed} is calculated by equation 3. All equations are extracted from CNR-DT 200 R1/2013.

$$G_F = k_b \cdot k_G \cdot \sqrt{f_{cm} \cdot f_{ctm}} = 0.077 \cdot \sqrt{48 \cdot 3.8} = 1.04 \frac{N}{mm} \tag{1}$$

$$F_{\max} = b_f \cdot \sqrt{2 \cdot E_f \cdot t_f \cdot G_f} = 40 \cdot \sqrt{2 \cdot 238000 \cdot 0.125 \cdot 1.04} = 9.95 kN \tag{2}$$

$$l_{ed} = \frac{1}{f_{bd}} \cdot \sqrt{\frac{\pi^2 \cdot E_f \cdot t_f \cdot G_f}{2}} = \frac{s_u (= 0.25mm)}{2 \cdot G_F} \cdot \sqrt{\frac{\pi^2 \cdot E_f \cdot t_f \cdot G_f}{2}} = 47\,mm \tag{3}$$

It will be noted that F_{max} is the 97 percentage of the "real" maximal bearable load. Thus, F_{max} could be set to F_{max} = 10.28 kN. Due to the high forces in the experiments with the epoxy and deformations/rotations of specimens for loads > 8 kN, the maximal measured force was limited to 8.3 kN. Nonetheless, almost all the experiments with PU are characterized by a low coefficient of variation. Furthermore, the experiments with 40 mm bonded length showed an almost constant distribution of bond stresses over the bonded length, so the approach to infer the local bond-slip laws as Walendy et al. (2017) did in their work is here reasonable, too.

2.3 Local bond stress-slip laws

The inferred local bond slip laws of PU 2 and PU 3, their simplified bilinear law and the corresponding fracture energies G_F are shown in figure 4. Tests were performed with a bonded length of 40 mm. The fracture energy is calculated by equation 4:

$$G_F = \int_0^{s_{max}} \tau(s) ds \tag{4}$$

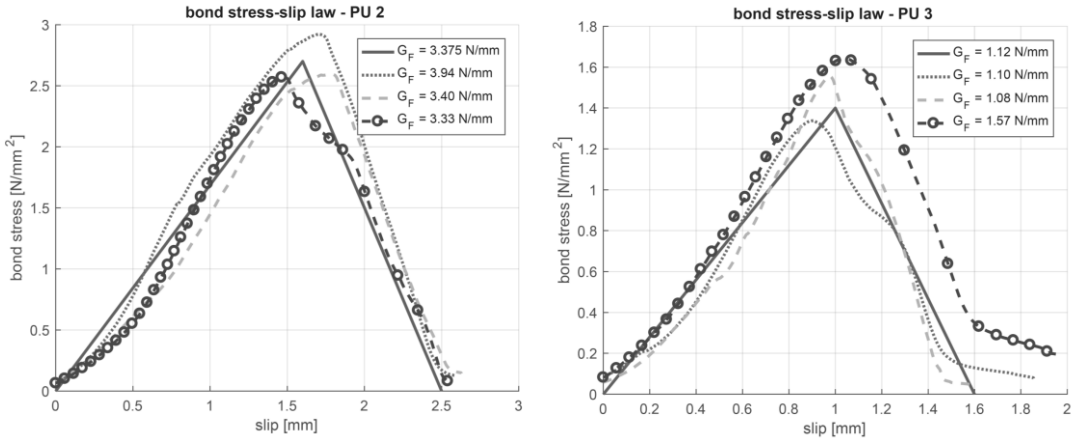

Figure 4. local bond-slip laws (experiments) and mean bilinear local bond slip law (solid line) of PU 2 and PU 3.

Remarkable are the high values of the fracture energy G_F and the ductility for PU 2 and PU 3, especially compared to the state-of-the-art adhesives, like the epoxy. Furthermore, the bond stress-slip laws are characterized by a reduced peak value of bond stress and much higher values of corresponding slips, which leads to a reduction of local bond (or shear) stresses and more evenly distributed stresses along the bonded area. This effect was mentioned by Fitton et al. (2005), Derkowski et al. (2010) and Kwiecień (2014) before. Moreover, Derkowski et al. (2010) showed in their experiments with strengthened RC beams, that FRP strengthening with a more flexible adhesive reduces the deflections of the beams compared to strengthening with stiffer adhesives. Thanks to those two issues, it could be possible to increase the debonding load to prevent early failure in the service limit state (SLS) and to change the failure mode from cohesion to adhesion failure. This could be a welcome side effect of the new approach, repair after failure is easier due to the not so much destroyed top surface of concrete cover (or the complete cover as a whole).

3 NUMERICAL WORK

The effect of the differing bond-slip laws on the load-bearing behavior is examined numerical in the next chapter with a MATLAB® algorithm. Due to the inferior maximum forces of PU 1 and PU 3 the following work focuses on the comparison of the FRP bonded with epoxy resins and PU 2. For this purpose calculations for increasing bond lengths (40 mm ÷ 400 mm) for PU 2 are performed and compared to the FRPs bonded with epoxy. All calculations are validated with the algorithm discussed in Walendy et al. (2017).

3.1 MATLAB® algorithm

The aim of the numerical work was to implement the inferred local bond-slip laws and to calculate loads, strains and stresses in the FRP over the bonded length. To get this results the differential equation:

$$s'' = \frac{\tau(s)}{E_L \cdot t_L} \tag{5}$$

had to be solved with a finite difference code that implements the three-stage Lobatto IIIa formula. This is a collocation formula and the collocation polynomial provides a C1-continuous solution that is fourth-order accurate uniformly in the integration area (bonded length). Two input values are used: strain of textile at the end of the bonded length (assumed to zero) and the value of slip at the loaded end (increased with every step). To verify the accuracy of the algorithm, calculated force-slip curves for 40 mm and 80 mm bonded length and PU 2 are shown in figure 5 and compared to the experimental curves.

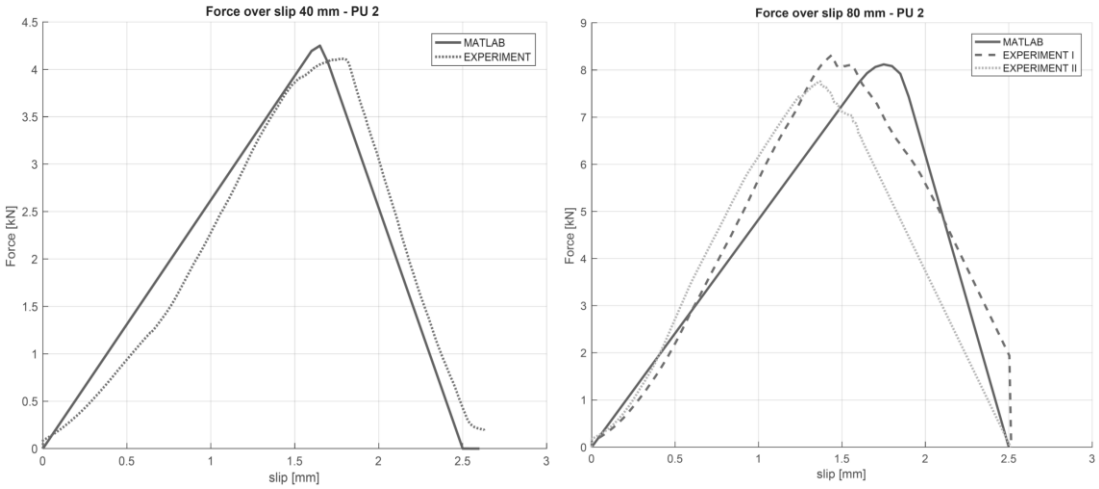

Figure 5. PU 2: force-slip curves for 40 mm (left) and 80 mm (right) bonded length.

3.2 force-slip curves for increasing bond length

Using the results (maximum bond stress f_{bd} and fracture energy G_F) of the tests of PU 2 (figure 4, left), the optimal bond length, according to CNR-DT 200 R1/2013, is set to

$$l_{ed} = \frac{1}{f_{bd}} \cdot \sqrt{\frac{\pi^2 \cdot E_f \cdot t_f \cdot G_f}{2}} = \frac{1}{2.70} \cdot \sqrt{\frac{\pi^2 \cdot 238000 \cdot 0.125 \cdot 3.375}{2}} = 261mm \quad (6)$$

Due to this very long required bond length, calculations for 40, 60, 80, 160, 300 and 400 mm bonded length were performed. The force-slip curves are shown in figure 3. In addition, two calculated curves for a FRP bonded with an epoxy resin and a bonded length of 80 mm are represented. Due to the much stiffer bond stress-slip law, their force-slip curves differ strongly from the curves of the FRP bonded with PU 2. Remarkable is the maximum debonding force F_{max} for PU 2 (MATLAB = 17.78 kN / CNR-DT = 17.93 kN) compared to epoxy bonded FRPs (10.28 kN). Reasons for the deviation of maximal loads from 300 mm and 400 mm are some numerical inaccuracies due to the singularity of the bond stress-slip relationship at the peak bond stress and ultimate slip. The deviation is only 2.7 %.

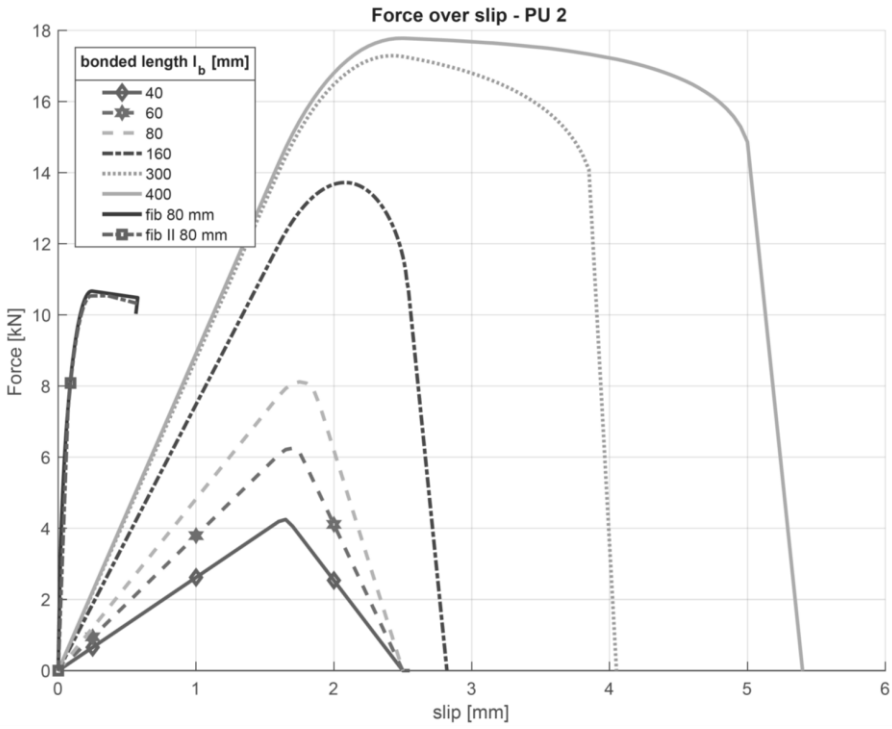

Figure 6. calculated force-slip curves of FRP bonded with PU 2 and epoxy (fib & fib II) for different bonded lengths.

The distribution of bond stresses over a large area is the key to increase the ultimate load of the FRP strengthening system. This can be shown in figure 7. Shown is the force over slip curve for a bonded length of 400 mm and PU 2. For three selected points A, B and C the bond stress distribution over the bonded length is shown. Already at a load level of $0.67 \cdot F_{max}$ the bond stresses (and slips) are distributed over a quite large area. Carloni (2014) determined the size of the stress transfer zone (STZ) to ≈ 65 mm (epoxy adhesive). In the case of PU the STZ is about 260 mm - 300 mm. This is a major difference to the epoxy based strengthening systems. This difference is becoming more important for the strengthening of low strength concrete parts due to the reduction of peak bond stresses and the activation of a larger bonded area.

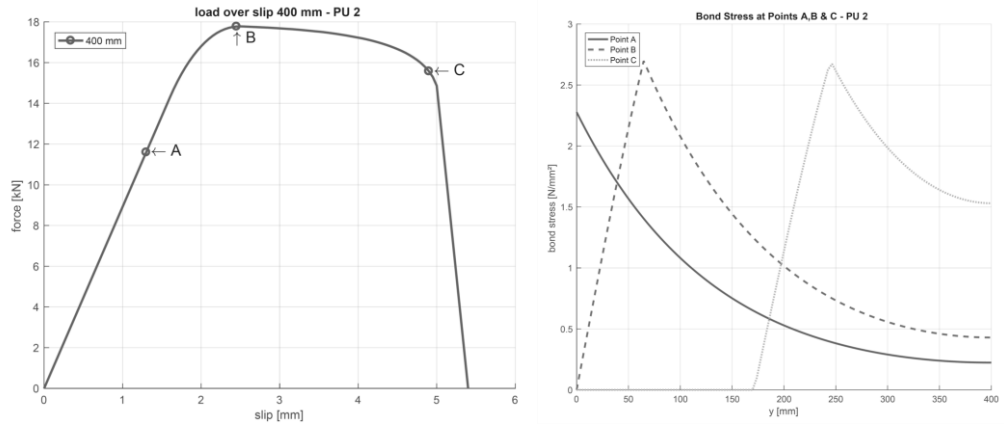

Figure 7. force-slip curves for PU 2 / 400 mm bonded length and corresponding bond stresses over bonded length for points A, B (maximum load) and C.

4 CONCLUSIONS

The experimental und numerical work outlined in this paper showed the potential for optimization by the use of a softer adhesive for strengthening RC structures with FRPs. A softer adhesive reduces the peak (bond) stresses occurring at cracks and increase the effective bond length. Due to the increased bond length, the bond stresses are more evenly distributed, a larger area of the bonded surface is activated and the debonding load is increased. In this work, three different polyurethans (PU) were tested and one of them seems to be promising. The PU 2 is characterized by a reduced peak bond stress and ultimate slips factor 10 higher than nowadays used epoxy resins. As a result of those characteristics, the fracture energy G_F is increased and the ultimate (debonding) load as well. Further research on this topic will be carried out, important issues are the improvement of the bond to the concrete surface, creep resistance and endurance of the strengthening system as a whole.

5 REFERENCES

CNR-DT 200 R1/2013 – Guide for the Design and Construction of Externally Bonded FRP Systems for Strengthening Existing Structures.

Carloni, C., 2014, Analyzing bond characteristics between composites and quasi-brittle substrates in the repair of bridges and other concrete structures, *Advanced Composites in Bridge Construction and Repair (Woodhead Publishing Series in Civil and Structural Engineering), 1st Edition*, 61-93.

Derkowski, W., A. Kwiecień, B. Zając, 2010, Comparison of CFRP strengthening efficiency of bent RC elements using stiff and flexible adhesives, *3rd International fib Congress and PCI Convention*, Washington D.C., USA.

Derkowski, W., A. Kwiecień, B. Zając, 2013, CFRP strengthening of bent RC Beams using stiff and flexible adhesives, *Technical transactions 1-B/2013*, 37-52.

Fitton, M.D., J.G.Broughton, 2005, Variable modulus adhesives: an approach to optimized joint performance, *International Journal of Adhesion & Adhesives*, 25.

Kwiecień, A., 2014, Shear bond of composites-to-brick applied with highly deformable, in relation to epoxy resin, interface materials, *Materials and Structures*, 47, 2005-2020.

Walendy, B., R. Sedlmair, L. Stempniewski, 2017, Standardization approach for a new class of retrofitting systems, *SMAR 2017 – fourth International Conference on Smart Monitoring, Assessment and Rehabilitation of Civil Structures, conference paper*, Zurich, Switzerland.